Journal of Materials Science and Chemical Engineering, 2025, 13(8), 55-65
https://www.scirp.org/journal/msce
ISSN Online: 2327-6053
ISSN Print: 2327-6045

Dynamic Analysis of Thermo-Magnetic Effects on a $N^+/P/P^+$ Silicon Solar Cell

Sada Traore[1,2], Ansoumane Diedhiou[2], Moustapha Thiame[2], Modou Tine[2], Moussa Camara[2], Landing Diatta[2]

[1]Laboratory of Semiconductors and Solar Energy, Physics Department, Faculty of Science and Technology, University Cheikh Anta Diop, Dakar, Senegal
[2]LCPM Laboratory, Department of Physics, Assane Seck University of Ziguinchor, Ziguinchor, Senegal
Email: sadatraore59@yahoo.fr

How to cite this paper: Traore, S., Diedhiou, A., Thiame, M., Tine, M., Camara, M. and Diatta, L. (2025) Dynamic Analysis of Thermo-Magnetic Effects on a $N^+/P/P^+$ Silicon Solar Cell. *Journal of Materials Science and Chemical Engineering*, **13**, 55-65.
https://doi.org/10.4236/msce.2025.138005

Received: July 25, 2025
Accepted: August 18, 2025
Published: August 21, 2025

Abstract

In this study, we analyze the dynamic behaviour of a silicon solar cell with an $N^+/P/P^+$ structure subjected simultaneously to thermal and magnetic stresses. The theoretical approach is based on solving the diffusion equation in the frequency domain, incorporating the effects of temperature and magnetic field on minority carriers. The influence of these factors on mobility, diffusion coefficient, surface recombination, and electrical performance (Jsc, Voc, impedance) is examined in detail. Frequency-domain analysis, particularly through Nyquist plots, reveals alterations in capacitive and resistive properties, modelled using a modified Randles equivalent circuit. These results provide in-depth insight into dynamic losses caused by extreme environments and offer pathways for optimizing the design of robust solar cells suited for space, industrial, or embedded applications.

Keywords

Complex Impedance, Magnetic Field, Temperature, Nyquist Plot, Extreme Environment

1. Introduction

In extreme environments such as Sahelian regions, industrial applications, or space, photovoltaic (PV) cells are subjected to significant thermal variations and magnetic fields that can disrupt internal charge transport mechanisms [1]-[3]. These effects influence the transport and recombination of minority carriers, which in turn impact the overall performance of the solar cell. [4] [5]. Studies conducted in Senegal have highlighted the need to adapt PV cells to such conditions. Dialo *et al.* [5] demonstrated the impact of climatic factors on the

electrical parameters of a silicon module in Dakar. Mohamed *et al.* [6], Thiaw *et al.* [7], and Teya *et al.* [8] analyzed the combined influence of magnetic field and temperature on the static and dynamic characteristics of $N^+/P/P^+$-type cells.

In this context, the present work aims to develop a thermo-magnetic-frequency modelling of a silicon $N^+/P/P^+$ cell, an architecture widely used for its robustness and ease of fabrication. The main objective is to analyze the combined influence of temperature and a magnetic field on the dynamic behavior of the cell in the frequency domain, focusing specifically on: the diffusion coefficient and carrier mobility; the rear surface recombination velocity; the Short-circuit current density (Jsc) and open-circuit voltage (Voc) parameters; and the complex impedance analyzed via Bode and Nyquist plots.

The methodology is based on solving the frequency-modulated diffusion equation, incorporating the effects of the Lorentz force due to the magnetic field, as well as thermal variations in carrier lifetime, diffusivity, and mobility. Additionally, an equivalent electrical model is developed to represent the capacitive and resistive losses induced by these environmental stresses, thereby providing a simplified yet accurate representation of the cell's behavior under dynamic conditions.

2. Theory and Modelling

2.1. Structure of the $N^+/P/P^+$ Solar Cell

The solar cell under study is composed of silicon layers forming a structure known as $N^+/P/P^+$. It operates under polychromatic light (composed of multiple wavelengths) and is analyzed under time-varying operating conditions, referred to as frequency-domain dynamic operation. The key physical phenomena occur in the central layer, known as the base (P-type), where electrons are generated by light, diffuse through the material, and may recombine.

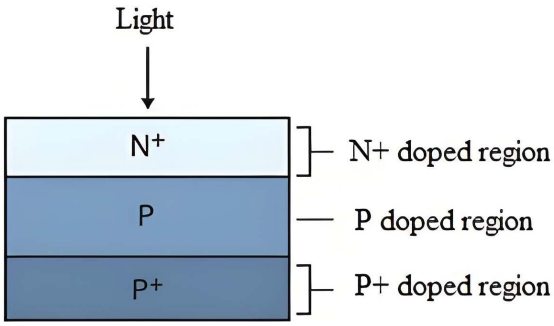

Diagram 1. Structure of the silicon solar cell ($N^+/P/P^+$).

2.2. Mathematical Model of the $N^+/P/P^+$ Solar Cell

2.2.1. Diffusion Equation (Minority Carriers in the P-Type Base)

The minority carrier density equation is given as follows.

$$\frac{\partial \delta n(x,t)}{\partial t} = D_n(\omega)\frac{\partial^2 \delta(x,t)}{\partial x^2} - \frac{\delta(x,t)}{\tau n} + G(x,t) \quad (1)$$

Where $D_n(\omega)$, is the effective diffusion coefficient in the frequency domain and is given by the following relation:

$$D_n^*(\omega) = \frac{D_n}{1 + j\omega\tau} \tag{2}$$

τn is the minority carrier lifetime, $\delta n(x,t)$ the excess electron density, and $G(x,t)$ the carrier generation rate due to illumination.

The expressions for $\delta n(x,t)$ and $G(x,t)$ are given by the following relations [9]:

$$\delta n(x,t) = \delta n(x) \cdot e^{j\omega t} \text{ et } G(x,t) = G(x) \cdot e^{j\omega t} \tag{3}$$

Where $\delta(x)$ and $g(x)$ represent the spatial components, and $e^{j\omega t}$ represents the temporal component. For this type of solar cell, the spatial component of the minority carrier generation rate is given by expression (4):

$$\delta(x,\omega) = A\cosh\left(\frac{x}{L(\omega)}\right) + B\sinh\left(\frac{x}{L(\omega)}\right) - \sum_{i=1}^{3} \beta_j \cdot e^{-\alpha x} \tag{4}$$

Where $L(\omega)$ is the complex diffusion length as a function of the modulation frequency, given by:

$$L(\omega) = \sqrt{\frac{D_n \tau_n}{1 + j\omega\tau}} \tag{5}$$

The constants A and B are determined from the boundary conditions at the junction and the back surface [10].

2.2.2. Boundary Conditions

- At the junction: $x = 0$

$$\left.\frac{\delta(x,\omega)}{\partial x}\right|_{x=0} = \frac{Sf}{D(\omega)}\delta(0,\omega) \tag{6}$$

- At the rear face: $x = H$

$$\left.\frac{\delta(x,\omega)}{\partial x}\right|_{x=H} = -\frac{Sb}{D(\omega)}\delta(H,\omega) \tag{7}$$

Where, *Sf* is the recombination velocity at the junction of excess minority carriers, and also determines the operating point of the photovoltaic cell [11]-[13]. *Sb* is the recombination velocity at the back surface of excess minority carriers [13] [14].

2.3. Relationship between Rear-Surface Recombination Rate and Minority Carrier Mobility in the Base

The expression for the recombination velocity at the rear surface (*Sb*) is determined from the derivative of the photocurrent density (*Jph*) with respect to the recombination velocity at the junction (*Sf*). For large values of *Sf* (*Sf* ≥ 10^6 cm/s), corresponding to a region where the photocurrent density curves become asymptotic with a zero gradient, we have:

$$\frac{\partial Jph(Sf,w,B,T,\Phi)}{\partial Sf}=0 \tag{8}$$

Solving this equation leads to two distinct expressions for the recombination rate at the back surface, denoted Sb_1 and Sb_2 [6].

$$Sb_1(w,B,T,\Phi) = \frac{D(w,B,T,\Phi)}{L(w,B,T,\Phi)}\sum_{i=1}^{3}\frac{\sinh\left(\frac{H}{L(w,B,T,\Phi)}\right)-L(w,B,T,\Phi)b_1\left[\cosh\left(\frac{H}{L(w,B,T,\Phi)}\right)-e^{-bH}\right]}{L(w,B,T,\Phi)b_1\sinh\left(\frac{H}{L(w,B,T,\Phi)}\right)-\left[\cosh\left(\frac{H}{L(w,B,T,\Phi)}\right)-e^{-bH}\right]} \tag{9}$$

$$Sb_2(w,B,T,\Phi) = -\frac{D(w,B,T,\Phi)}{L(w,B,T,\Phi)}\cdot\tanh\left(\frac{H}{L(w,B,T,\Phi)}\right) \tag{10}$$

In our study, and in order to simplify the calculation, we used the expression for Sb_2 to determine the explicit relationship between mobility (equation 11) and the geometric (H), magnetic (B), thermal (T), and optical (Φ) parameters.

$$\mu(\omega,B,T,\Phi,H) = -q\frac{Sb(\omega,B,T,\Phi)\cdot L_\omega(\omega,B,T,\Phi)}{K_b\cdot T}\frac{1}{\tanh\left(\frac{H}{L_\omega(\omega,B,T,\Phi)}\right)} \tag{11}$$

3. Results

3.1. Calibration of Magnetic Field and Temperature Values

As part of the study on charge carrier transport in a photovoltaic cell subjected to a magnetic field, it is crucial to understand how thermal and magnetic parameters influence diffusion mechanisms. The diffusion coefficient, denoted D, is a fundamental parameter that describes the mobility of minority carriers, especially in dynamic regimes where operating conditions deviate from equilibrium. To properly calibrate the values of the magnetic field B and the temperature T used in the modeling, a preliminary analysis was conducted to evaluate their combined effect

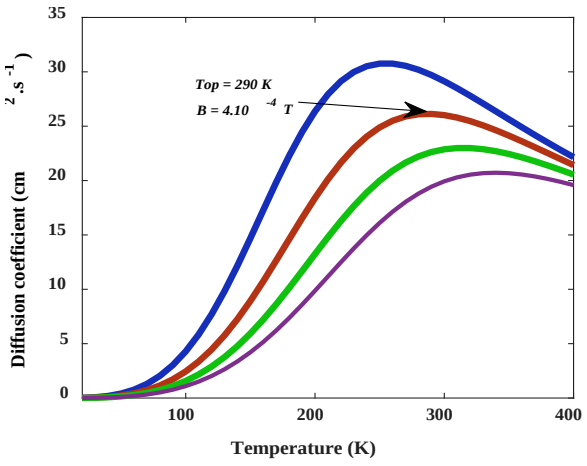

Figure 1. Diffusion coefficient as a function of temperature.

on the diffusion coefficient. Figure 1 shows the variation of the minority carrier diffusion coefficient D as a function of temperature, for different magnetic field intensities ranging from $3 \times 10^{-4} T$ to $10^{-3} T$.

This modeling makes it possible to identify the optimal temperature range for each magnetic field intensity, which is crucial for maximizing the efficiency of solar cells in varying environments.

3.2. Thermomagnetic Effect on Back Surface Recombination Velocity

The performance of a solar cell is strongly influenced by the recombination of minority carriers, particularly at the back surface, where passivation is generally more challenging. In this context, the present modeling focuses on evaluating the combined impact of temperature T and magnetic field B on the back surface recombination velocity Sb, as a function of the charge carrier mobility μ. Figure 2 presents the simulated results of the magnitude of the recombination velocity Sb as a function of mobility μ for different temperature and magnetic field values. Each curve shows an increasing linear trend, indicating a proportional relationship between μ and Sb, which means that as mobility increases, surface recombination becomes more significant.

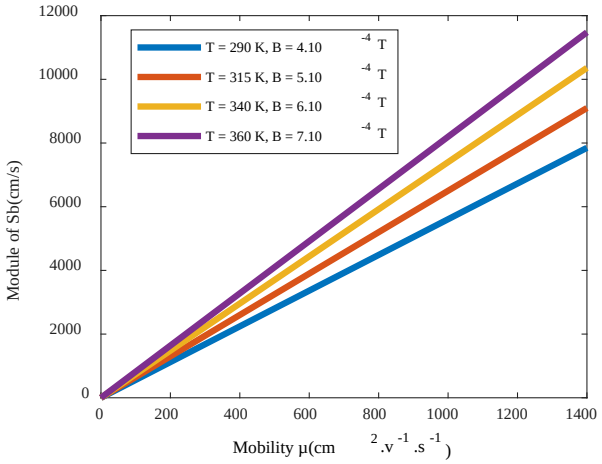

Figure 2. Recombination velocity Sb as a function of mobility μ for different temperature and magnetic field values.

The curves also reveal that, for the same mobility μ, the recombination velocity Sb increases with both temperature and magnetic field. This indicates that at high temperatures, thermal agitation enhances carrier recombination. Furthermore, under stronger magnetic fields, the Lorentz force alters the trajectories of charge carriers, which can increase recombination losses especially in regions with a strong field gradient.

3.3. Effect of Magnetic Field and Temperature on Short-Circuit Current Density (Jsc) and Open-Circuit Voltage (Voc)

Figure 3 illustrates the combined effect of the magnetic field B and temperature

T on two key electrical parameters of solar cells: the short-circuit current density Jsc and the open-circuit voltage Voc.

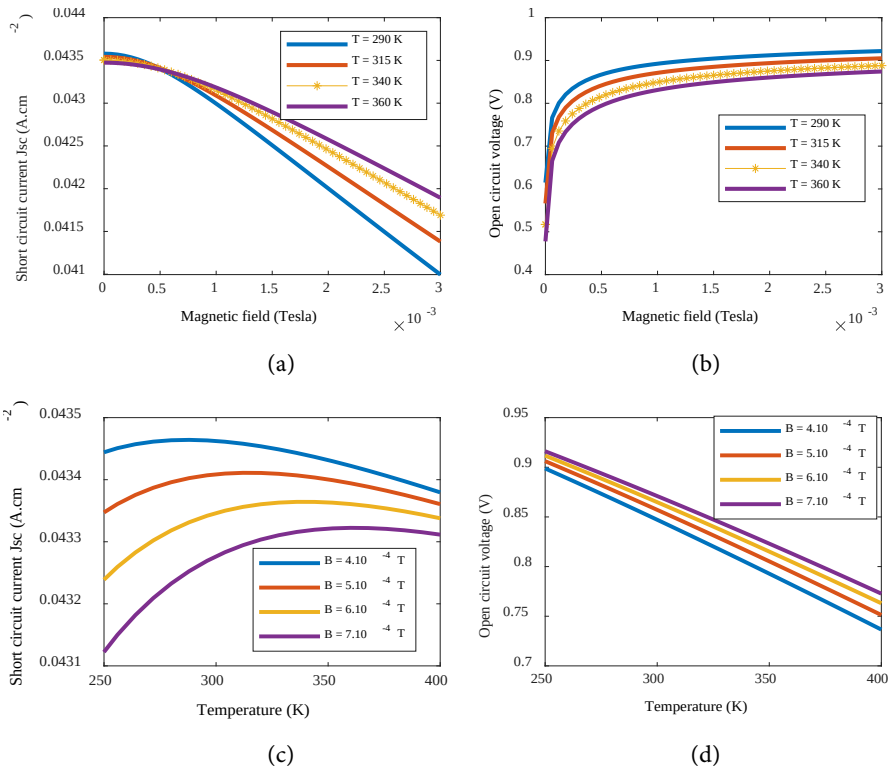

Figure 3. Variation of Jsc and voc as a function of magnetic field (a) and (b) and temperature (c) and (d).

The analysis of the variations in short-circuit current density (Jsc) and open-circuit voltage (Voc) reveals the following: the short-circuit current density (Jsc) decreases with increasing magnetic field due to the Lorentz force acting on carrier trajectories. Similarly, the open-circuit voltage (Voc) also decreases with the magnetic field *B*, albeit more moderately. Temperature has a dual effect: it initially increases Jsc due to enhanced thermal generation, but ultimately degrades it beyond a certain threshold as recombination processes become dominant. In contrast, Voc continuously decreases with temperature *T*, in line with the classical theory of PN junctions. Overall, this modeling highlights the importance of accounting for the coupled effects of magnetic field (*B*) and temperature (*T*) in the design and performance prediction of solar cells intended for extreme environments (e.g., space, industrial settings, integrated magnetic sensors). It also emphasizes the need to optimize surface passivation, thermal management, and the selection of materials with high magneto-thermal robustness, as well as the design of more resilient structures (e.g., magnetic shielding, passive cooling, and low-recombination materials).

3.4. Frequency Analysis of Impedance

his section presents the frequency-domain study of the dynamic behavior of a sil-

icon solar cell subjected to varying magnetic fields. The analysis is based on the evolution of the phase of the complex impedance $Z(\omega)$ (**Figure 4(a)**) and its representation in the complex plane (Nyquist diagram, **Figure 4(b)**). It highlights delayed transport mechanisms as well as capacitive and resistive effects induced by the physical parameters of the system.

3.4.1. Effect of the Magnetic Field

Figure 4 analyzes the frequency-dependent behavior of the complex impedance $Z(\omega)$ of a silicon solar cell under different magnetic field strengths.

Figure 4(a) shows that the impedance phase exhibits a minimum located in the range $\log(\omega) \in [6,7]$. This range corresponds to the system's relaxation resonance frequency, where capacitive and resistive effects temporarily balance each other. As the magnetic field B increases, a more pronounced phase shift (*i.e.*, a more negative phase) is observed, indicating slower carrier dynamics, charge accumulation, or increased interfacial resistance.

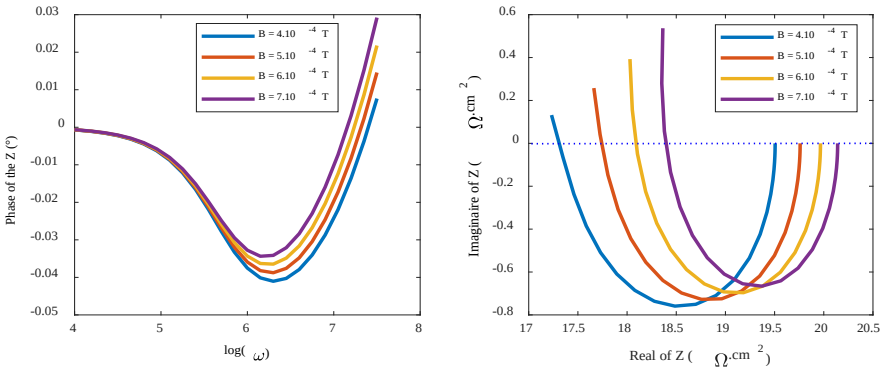

(a) (b)

Figure 4. Frequency response of the impedance under magnetic field. (a) Phase analysis, (b) Complex impedance analysis—Nyquist diagram.

In **Figure 4(b)** we also observe semi-circular curves typical of RC type response systems. As the magnetic field (B) increases, the real part of the impedance (Z) shifts toward higher values, indicating an increase in series resistance (Rs) or recombination resistance (Rp). Similarly, the imaginary part of (Z) reaches more negative minimum values, suggesting enhanced junction or diffusion capacitance. The widening of the arcs further reveals a dispersion in time constants, linked to the non-uniformity of recombination processes under the magnetic field.

These results demonstrate the influence of the magnetic field on the global capacitive and resistive behavior of the cell, reflecting a degradation in carrier collection dynamics and a modification of the junction properties.

3.4.2. Effect of Temperature

Figure 5 shows the evolution of the phase (**Figure 5(a)**) and the complex impedance (**Figure 5(b)**) as a function of frequency for different temperatures. The phase exhibits a minimum around $\log(\omega) \approx 6$, indicating capacitive behavior,

slightly modulated by temperature.

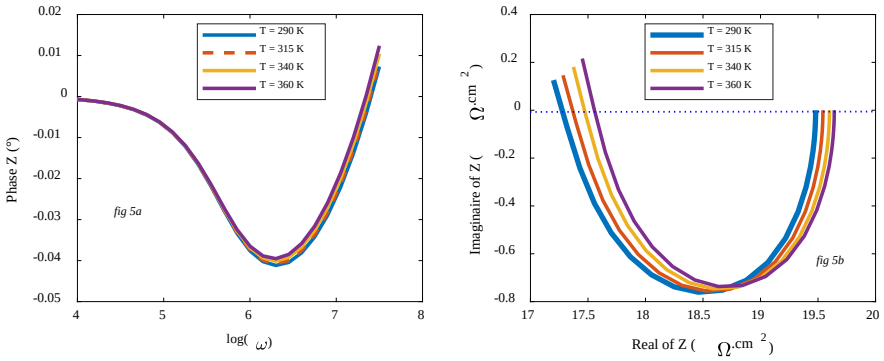

(a) (b)

Figure 5. Variation of the phase (a) and of the real and imaginary parts of the impedance (b) as a function of frequency for different temperatures.

The Nyquist diagrams (**Figure 5(b)**) reveal depressed arcs, indicating non-ideal behavior typical of a distributed RC circuit. As temperature increases, the real part of the impedance decreases, suggesting a reduction in internal resistance due to improved carrier mobility or a lowering of recombination barriers. These results highlight the thermal impact on transport mechanisms within the solar cell.

3.4.3. Combined Effect of Magnetic Field and Temperature

The Nyquist diagram presented illustrates the evolution of the complex impedance as a function of both temperature and applied magnetic field (**Figure 6**). The typical semi-circular behavior can be modeled by an equivalent electrical circuit consisting of a series resistance Rs in series with a parallel branch composed of a resistance Rp and capacitance C. He is equivalent to (Rs + (Rp // C).

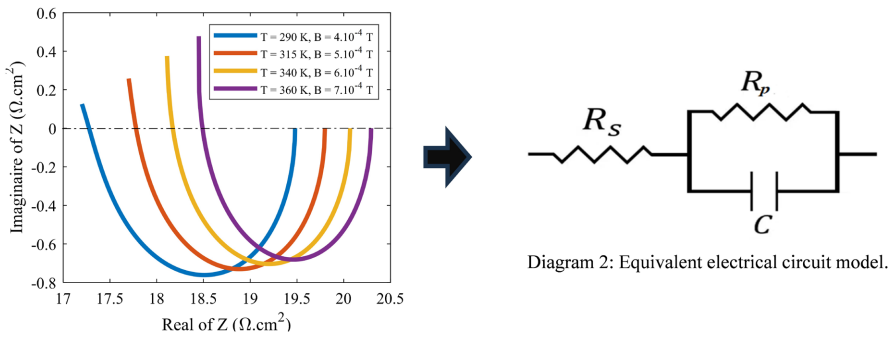

Diagram 2: Equivalent electrical circuit model.

Figure 6. Nyquist diagrams of the measured complex impedance for different temperatures and applied magnetic field intensities.

An increase in the series resistance (Rs) and a slight decrease in the parallel resistance (Rp) are observed with rising temperature and magnetic field intensity.

The increase in Rs with temperature and magnetic field indicates a reduction in carrier mobility. Simultaneously, the decrease in Rp reflects an increase in recombination or internal losses, while the capacitance C varies depending on charge

accumulation at the interface. This model enables a detailed analysis of transport phenomena under thermo-magnetic effects.

These results confirm that thermo-magnetic coupling significantly affects transport and recombination mechanisms in photovoltaic structures and highlight the relevance of frequency analysis as a diagnostic tool for characterizing internal phenomena under multiple external stresses.

4. Conclusions

In this study, we developed a comprehensive model of the dynamic behavior of an $N^+/P/P^+$ silicon solar cell subjected to simultaneous thermal and magnetic field stresses. The theoretical and numerical approach, based on solving the diffusion equation in the frequency domain, allowed us to quantify the impact of thermo-magnetic coupling on fundamental transport mechanisms mobility, diffusion, surface recombination as well as on the cell's electrical performance (Jsc, Voc, impedance).

The frequency analysis using Nyquist plots and the equivalent circuit modeling based on a modified Randles model revealed the direct influence of these stresses on capacitive and resistive losses. Specifically, the increase in temperature and magnetic field leads to a rise in series resistance and an intensification of recombination processes, indicating a progressive degradation in carrier dynamics.

This work provides a rigorous and generalizable analytical framework for studying photovoltaic cells operating in extreme environments, incorporating effects that have so far been overlooked in classical models.

These findings pave the way for the development of more robust devices for extreme conditions, integrating thermal management and magnetic shielding strategies, and tailored to meet the demands of space, industrial, or embedded technologies.

However, although this study is based on a theoretical approach grounded in solid physical principles and supported by numerical simulations, experimental validation remains necessary to confirm its relevance under real-world conditions. Future research should therefore focus on conducting controlled experiments or in-situ measurements to test and refine the proposed model under thermo-magnetic constraints.

Conflicts of Interest

The authors declare no conflicts of interest regarding the publication of this paper.

References

[1] Diouf, B. and Pode, R. (2013) Initiative for 100% Rural Electrification in Developing Countries: Case Study of Senegal. *Energy Policy*, **59**, 926-930. https://doi.org/10.1016/j.enpol.2013.04.012

[2] Mane, R., Ly, I., Wade, M., Datta, I., Douf, M., Traoré, Y., Ndiaye, M., Tamba, S. and Sissoko, G. (2017) Minority Carrier Diffusion Coefficient D (B, T): Study in Temper-

ature on a Silicon Solar Cell under Magnetic Field. *Energy and Power Engineering*, **9**, 1-10. http://www.scirp.org/journal/epe
https://doi.org/10.4236/epe.2017.91001

[3] Combari, D., Zerbo, I., Zoungrana, M., Ramde, E. and Bathiebo, D. (2017) Modelling Study of Magnetic Field Effect on the Performance of a Silicon Photovoltaic Module. *Energy and Power Engineering*, **9**, 419-429. http://www.scirp.org/journal/epe
https://doi.org/10.4236/epe.2017.98028

[4] Dione, B., Boiro, M. and Thiam, M.F. (2022) Influence of Temperature on the Serial and Shunt Resistance of a Silicon Solar Cell under Polychromatic Illumination in Static Mode. *IRA-International Journal of Applied Sciences* (*ISSN 2455-4499*), **17**, 51-60. https://doi.org/10.21013/jas.v17.n4.p3

[5] Diop, D., Diagne, M., Sambou, A., Bassene, P.D., Niang, S.A.A. and Sarr, A. (2021) Influence of Dust Soiling on the Electrical Parameters of Silicon-Based Photovoltaic Panel in Dakar, Senegal. *Energy and Power Engineering*, **13**, 174-189.
https://www.scirp.org/journal/epe
https://doi.org/10.4236/epe.2021.135012

[6] Mohamed, N.M.M.O., Sow, O., Gueye, S., Traore, Y., Diatta, I., Thiam, A., Ba, M.A, Mane, R, Ly, I. and Sissoko, G. (2019) Influence of Both Magnetic Field and Temperature on Silicon Solar Cell Base Optimum Thickness Determination. *Journal of Modern Physics*, **10**, 1596-1605.
https://doi.org/10.4236/jmp.2019.1013105

[7] Thiaw, C., Ba, M. L., Ba., M.A., Diop, G., Diatta, I., Ndiaye, M. and Sissoko, G. (2020) N^+-P-P^+ Silicon Solar Cell Base Optimum Thickness Determination under Magnetic Field. *Journal of Electromagnetic Analysis and Applications*, **12**, 103-113.
https://doi.org/10.4236/jemaa.2020.127009

[8] Teya, M.Y., Sow, O., Loum, K., Diatta, I., Diop, G., Traore, Y., Wade, M. and Sissoko, G. (2023) Determination of the Base Optimum Thickness of Back-Illuminated (N^+/P/P^+) Bifacial Silicon Solar Cell by Help of Diffusion Coefficient at Resonance Frequency. *Journal of Electromagnetic Analysis and Applications*, **15**, 13-24.
https://doi.org/10.4236/jemaa.2023.152002

[9] Furlan, J. and Amon, S. (1985) Approximation of the Carrier Generation Rate in Illuminated Silicon. *Solid-State Electronics*, **28**, 1241-1243.
https://doi.org/10.1016/0038-1101(85)90048-6

[10] Sissoko, G., Museruka, C., Corréa, A., Gaye, I. and Ndiaye, A. L. (1996) Light Spectral Effect on Recombination Parameters of Silicon Solar Cell. *World Renewable Energy Congress*, Denver, 15-21 June 1996, 1487-1490.

[11] Sissoko, G., Dieng, B., Corréa, A., Adj, M. and Azilinon, D. (2004) Silicon Solar Cell Space Charge Region Width Determination by a Study in Modeling. *Renewable Energy*, **3**, 1852-1855.

[12] Barro, F.I., Nanéma, E., Werème, A., Zougmoré, F. and Sissoko, G. (2001) Bulk and Surface Recombination Measurement in Silicon Double Sided Surface Field Solar Cell under Constant White Bias Illumination. *Proceedings of the* 17*th European Photovoltaic Solar Energy Conference*, Munich, Munich, 22-26 October 2001, 368-371.

[13] Ndiaye, E., Sahin, G., Dieng, M., Thiam, A., Diallo, A.L., Ndiaye, M. and Sissoko, G. (2015) Study of the Intrinsic Recombination Velocity at the Junction of Silicon Solar Cell under Frequency Modulation and Radiation. *Journal of Applied Mathematics and Physics*, **3**, 1522-1535.
https://doi.org/10.4236/jamp.2015.311177

[14] Diallo, H.L., Seïdou Maiga, A., Wereme, A. and Sissoko, G. (2008) New Approach of

Both Junction and Back Surface Recombination Velocities in a 3D Modelling Study of a Polycrystalline Silicon Solar Cell. *The European Physical Journal Applied Physics*, **42**, 203-211. https://doi.org/10.1051/epjap:2008085